

AD-A107 268

NAVAL RESEARCH LAB WASHINGTON DC

F/G 17/9

LINEAR FREQUENCY MODULATION DERIVED POLYPHASE PULSE-COMPRESSION--ETC(U)

NOV 81 B L LEWIS, F F KRETSCHMER

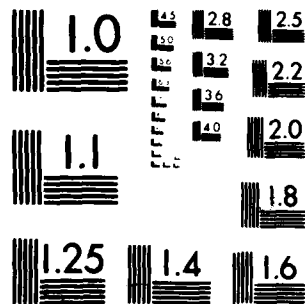
UNCLASSIFIED

NRL-8541

NL



END  
DATE  
FILMED  
12 81  
DTIC



MICROCOPY RESOLUTION TEST CHART  
NATIONAL BUREAU OF STANDARDS 1963 A<sub>1</sub>

01

② LEVEL II

NRL Report 5048

AD A107268

**Linear Frequency Modulation Derived  
Polynomial Pulse-Compression Codes and an  
Efficient Digital Implementation**

R. L. LUTZ AND R. P. KATZBERG, JR.  
Naval Electronics Research  
Development Center

November 2, 1961

DTIC  
ELECTE  
NOV 12 1961  
S D B

NO FILE COPY

(14) NRL-8541

SECURITY CLASSIFICATION OF THIS PAGE (When Data Entered)

REPORT DOCUMENTATION PAGE		READ INSTRUCTIONS BEFORE COMPLETING FORM
1. REPORT NUMBER NRL Report 8541	2. GOVT ACCESSION NO. AD-A107 268	3. RECIPIENT'S CATALOG NUMBER (9)
4. TITLE (and Subtitle) LINEAR FREQUENCY MODULATION DERIVED POLYPHASE PULSE-COMPRESSION CODES AND AN EFFICIENT DIGITAL IMPLEMENTATION		5. TYPE OF REPORT & PERIOD COVERED Interim report on continuing NRL problem (2)
6. PERFORMING ORG. REPORT NUMBER		7. CONTRACT OR GRANT NUMBER(s)
8. AUTHOR(s) B.L. Lewis and F.F. Kretschmer, Jr.		9. PROGRAM ELEMENT, PROJECT, TASK AREA & WORK UNIT NUMBERS 62712N; SF12141491; 53-0000-00
10. PERFORMING ORGANIZATION NAME AND ADDRESS Naval Research Laboratory Washington, D.C. 20375		11. REPORT DATE November 2, 1981
12. CONTROLLING OFFICE NAME AND ADDRESS Commander Naval Sea Systems Command Washington, D.C. 20362		13. NUMBER OF PAGES 10 (12) 21
14. MONITORING AGENCY NAME & ADDRESS (if different from Controlling Office)		15. SECURITY CLASS. (of this report) UNCLASSIFIED
16. DISTRIBUTION STATEMENT (of this Report) Approved for public release; distribution unlimited.		17. DECLASSIFICATION/DOWNGRADING SCHEDULE
18. DISTRIBUTION STATEMENT (of the abstract entered in Block 20, if different from Report)		
19. SUPPLEMENTARY NOTES		
20. KEY WORDS (Continue on reverse side if necessary and identify by block number) Radar Waveform Design Signal Processing		
21. ABSTRACT (Continue on reverse side if necessary and identify by block number) Two new polyphase pulse compression codes and efficient digital implementation techniques are presented that are very doppler tolerant and that can provide large pulse compression ratios. One of these codes is tolerant of precompression bandwidth limitations.		

251950

*[Signature]*

DD FORM 1473  
1 JAN 73

EDITION OF 1 NOV 65 IS OBSOLETE  
S/N 0102-014-6601

1/ii

SECURITY CLASSIFICATION OF THIS PAGE (When Data Entered)

## CONTENTS

INTRODUCTION .....	1
NEW PHASE CODES .....	1
P3 CODE .....	1
P4 CODE .....	2
EFFICIENT DIGITAL PULSE EXPANDER- COMPRESSOR IMPLEMENTATION .....	3
PERFORMANCE DATA .....	6
CONCLUSIONS .....	8
REFERENCES .....	8

Accession For	
NTIS	<input checked="" type="checkbox"/>
DTIC	<input type="checkbox"/>
Unannounced	<input type="checkbox"/>
Distribution	
Availability Codes	
Avail and/or	
Special	
<b>A</b>	

# LINEAR FREQUENCY MODULATION DERIVED POLYPHASE PULSE-COMPRESSOR CODES AND AN EFFICIENT DIGITAL IMPLEMENTATION

## INTRODUCTION

In previous publications [1,2], the authors introduced a new class of polyphase pulse-compression codes and techniques for use in digitally coded radars. Such codes and compressors can be employed to obtain much larger time-bandwidth products (pulse compression ratios) than are feasible with analog dispersive delay lines.

It is the purpose of this report to extend this class to include two new codes, one of which is tolerant of precompression bandwidth limitation [2].

These new phase codes are conceptually derived from a linear frequency modulation waveform (LFMW) and are more doppler tolerant than other phase codes derived from a step approximation to a LFMW. This report will also describe an efficient technique for implementing these new phase codes in a digital pulse-expander-compressor and will present performance data.

It should be noted that these phase codes are designed to be used both on transmission and reception to insure that the receive filter matches the transmitted waveform independent of time differences between the leading edge of the echo and a sampling pulse, i.e., independent of target range.

## NEW PHASE CODES

The two new phase codes will be called the P3 and P4 codes to distinguish them from the P1 and P2 codes discussed in Ref. 2. The P3 code is not precompression bandwidth limitation tolerant, but is much more doppler tolerant than the Frank [3] or P1 and P2 codes. The P4 code is a rearranged P3 code with the same doppler tolerance and with better precompression bandwidth limitation tolerance.

## P3 CODE

The P3 code is conceptually derived by converting a linear frequency modulation waveform to baseband using a local oscillator on one end of the frequency sweep and sampling the inphase I and quadrature Q video at the Nyquist rate. Assuming that the waveform to be coherently detected has a pulse length  $T$  and frequency

$$f = f_o + kt, \quad (1)$$

where  $k$  is a constant, the bandwidth of the signal will be approximately

$$B = kT. \quad (2)$$

Manuscript submitted August 20, 1981.

# LEWIS AND KRETSCHMER

This bandwidth will support a compressed pulse length of approximately

$$t_c \approx 1/B, \quad (3)$$

and the waveform will provide a pulse compression ratio of

$$\rho = T/t_c = BT \quad (4)$$

Assuming that the first sample of I and Q is taken at the leading edge of the waveform, the phases of successive samples taken  $t_c$  apart will be

$$\phi_i^{(P3)} = 2\pi \int_0^{(i-1)t_c} [(f_o + kt) - f_o] dt = \pi k(i-1)^2 t_c^2, \quad (5)$$

where  $i = 1, 2, \dots, \rho$ . From Eq. (2),  $k = B/T$  and from Eq. (3),  $t_c = 1/B$ . Therefore, Eq. (5) can be written as

$$\phi_i^{(P3)} = \pi(i-1)^2 / BT = \pi(i-1)^2 / \rho. \quad (6)$$

With  $\rho = 16$ , the P3 code modulo  $2\pi$  is

$i$	=	1	2	3	4	5	6	7	8
$\phi_i^{(P3)}$	=	0	$\frac{\pi}{16}$	$\frac{4\pi}{16}$	$\frac{9\pi}{16}$	$\pi$	$\frac{25\pi}{16}$	$\frac{4\pi}{16}$	$\frac{17\pi}{16}$
$i$	=	9	10	11	12	13	14	15	16
$\phi_i^{(P3)}$	=	0	$\frac{17\pi}{16}$	$\frac{4\pi}{16}$	$\frac{25\pi}{16}$	$\pi$	$\frac{9\pi}{16}$	$\frac{4\pi}{16}$	$\frac{\pi}{16}$

## P4 CODE

The P4 code is conceptually derived from the same waveform as the P3 code. However, in this case, the local oscillator frequency is set equal to  $f_o + kT/2$  in the I, Q detectors. With this frequency, the phases of successive samples taken  $t_c$  apart will be

$$\phi_i^{(P4)} = 2\pi \int_0^{(i-1)t_c} [(f_o + kt) - (f_o + kT/2)] dt = 2\pi \int_0^{(i-1)t_c} k(t - T/2) dt \quad (7)$$

or

$$\phi_i^{(P4)} = \pi k(i-1)^2 t_c^2 - \pi kT(i-1)t_c = \frac{\pi(i-1)^2}{\rho} - \pi(i-1). \quad (8)$$

# NRL REPORT 8541

With  $\rho = 16$ , the P4 code modulo  $2\pi$  is

$i$	=	1	2	3	4	5	6	7	8
$\phi_i^{(P4)}$	=	0	$\frac{17\pi}{16}$	$\frac{4\pi}{16}$	$\frac{25\pi}{16}$	$\pi$	$\frac{9\pi}{16}$	$\frac{4\pi}{16}$	$\frac{\pi}{16}$
$i$	=	9	10	11	12	13	14	15	16
$\phi_i^{(P4)}$	=	0	$\frac{\pi}{16}$	$\frac{4\pi}{16}$	$\frac{9\pi}{16}$	$\pi$	$\frac{25\pi}{16}$	$\frac{4\pi}{16}$	$\frac{17\pi}{16}$

It should be noted that the largest phase increments from code element to code element are on the two ends of the P4 code but are in the middle of the P3 code. Thus, the P4 code is more precompression bandwidth limitation tolerant than the P3 code. This follows since precompression bandwidth limitations average the code phase increments and would attenuate the P4 code on the ends and the P3 code in the middle as discussed in Ref. 2. The former increases the peak to side-lobe ratio of the compressed pulse while the latter decreases it.

## EFFICIENT DIGITAL PULSE EXPANDER-COMPRESSOR IMPLEMENTATION

The P3 and P4 codes can be implemented in a pulse expander-compressor employing digital fast-Fourier-transform circuits (FFT) [4] similar to those discussed for the Frank and P1 codes in Ref. 2. These expander-compressors take advantage of the fact that the P3 code only differs from the Frank code by  $\pi$  phase shifts every  $\rho^{1/2}$  code elements and by added phase increments from code element to code element that repeat every  $\rho^{1/2}$  samples. These added phase shifts are caused by the linear frequency shift during the time the equivalent Frank code frequency is constant. This difference between the P3 and Frank codes is illustrated in Table 1 through Table 4 for  $\rho = 16$ . The extra phase increments can be added to the  $\rho^{1/2}$  individual time samples in the FFT and their accumulated value  $\pi$  in the same time period that Frank code frequency exists can be added to the frequency port outputs of the FFT (illustrated in Figs. 1 and 2). (Note that even-number multiples of  $\pi$  need not be added since they are equivalent to zero phase shift).

Table 1 — P3 Code Matrix,  $\rho = 16$

0	$\frac{\pi}{16}$	$\frac{4\pi}{16}$	$\frac{9\pi}{16}$
$\pi$	$\frac{25\pi}{16}$	$\frac{4\pi}{16}$	$\frac{17\pi}{16}$
0	$\frac{17\pi}{16}$	$\frac{4\pi}{16}$	$\frac{25\pi}{16}$
$\pi$	$\frac{9\pi}{16}$	$\frac{4\pi}{16}$	$\frac{\pi}{16}$



LEWIS AND KRETSCHMER

Table 2 -- Adding  $\pi$  to Every Other Row  
of Table 1 and Subtracting Even  
Multiples of  $\pi$

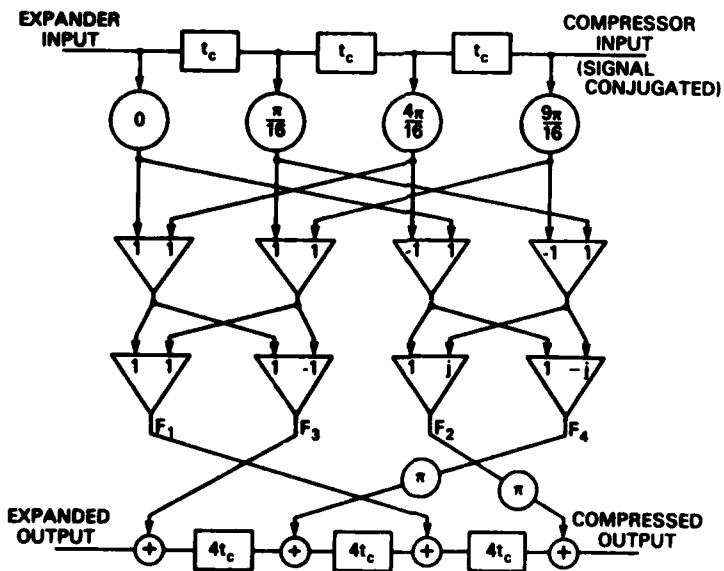
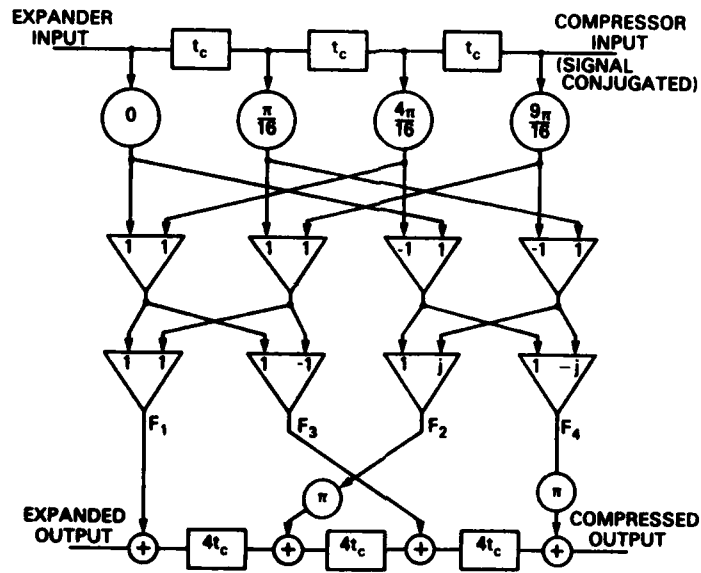
0	$\frac{\pi}{16}$	$\frac{4\pi}{16}$	$\frac{9\pi}{16}$
0	$\frac{9\pi}{16}$	$\frac{20\pi}{16}$	$\frac{\pi}{16}$
0	$\frac{17\pi}{16}$	$\frac{4\pi}{16}$	$\frac{25\pi}{16}$
0	$\frac{25\pi}{16}$	$\frac{20\pi}{16}$	$\frac{17\pi}{16}$

Table 3 -- Frank Code Matrix,  $\rho = 16$

0	0	0	0
0	$\frac{8\pi}{16}$	$\frac{16\pi}{16}$	$\frac{24\pi}{16}$
0	$\frac{16\pi}{16}$	0	$\frac{16\pi}{16}$
0	$\frac{24\pi}{16}$	$\frac{16\pi}{16}$	$\frac{8\pi}{16}$

Table 4 -- Subtracting Frank Code  
Phases (Table 3) from Phases  
in Table 2.

0	$\frac{\pi}{16}$	$\frac{4\pi}{16}$	$\frac{9\pi}{16}$
0	$\frac{\pi}{16}$	$\frac{4\pi}{16}$	$\frac{9\pi}{16}$
0	$\frac{\pi}{16}$	$\frac{4\pi}{16}$	$\frac{9\pi}{16}$
0	$\frac{\pi}{16}$	$\frac{4\pi}{16}$	$\frac{9\pi}{16}$



## PERFORMANCE DATA

Figure 3 illustrates the autocorrelation function or compressed-pulse waveform that is obtained with the digital pulse-expander-compressors illustrated in Figs. 1 and 2 with no doppler and no bandwidth limitation. The sample number corresponds to a range cell in time in a radar. In this case, the pulse-compression ratio is  $\rho = 100$  and the highest range-time sidelobe is  $4\rho$  below the peak response. For comparison purposes, Fig. 4 illustrates the autocorrelation function of the Frank or P1 codes with zero doppler and no bandwidth limitation — they both have 4-dB lower peak range-time sidelobes than the P3 or P4 codes.

Figure 5 illustrates the effect of a doppler shift equal to 5% of the bandwidth on the P3 or P4 code compressors. Figure 6 (for comparison purposes) shows the compressed pulse that would result from using the Frank or P1 codes with this doppler shift. Note that the large grating lobes that appear with doppler in the Frank or P1 code autocorrelation functions are absent in the P3 and P4 results.

The P3 and P4 code peak-gain cycles with increasing doppler like the Frank (and P1 and P2) code, as illustrated in Ref. 2, Fig. 1. This cycling repeats at doppler shifts equivalent to an odd multiple of a half-range-cell range-doppler coupling, i.e., when the doppler causes  $\pi$  phase shift across the uncompressed pulse. These gain changes and the accompanying peak broadening can be controlled by amplitude weighting the FFT frequency ports in the compressor on receive, as discussed in Ref. 1.

With large doppler shifts, as shown in Fig. 5, all frequency derived polyphase-pulse-compression-code autocorrelation functions are folded in frequency due to the time sampling. This folding produces the asymmetry in the farthest out sidelobes. An up doppler makes the highest frequency part of the code match the lowest frequency part of the matched filter, while down doppler produces a reverse effect.

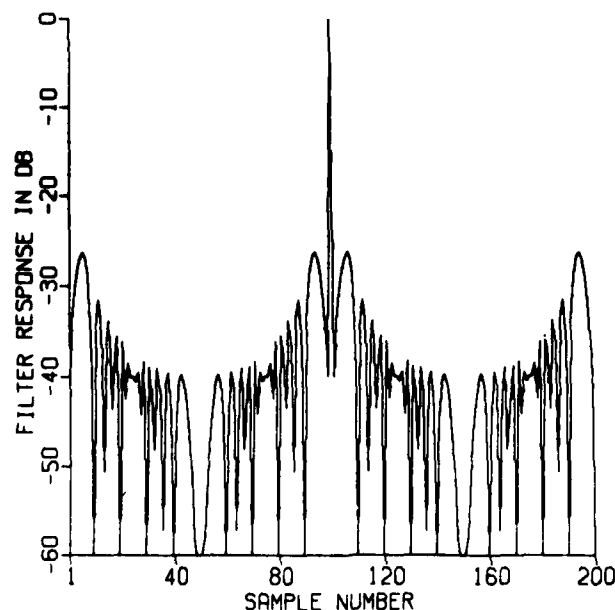


Fig. 3 — P3 or P4 autocorrelation function,  $\rho = 100$ , zero doppler shift and no bandwidth limitation

NRL REPORT 8541

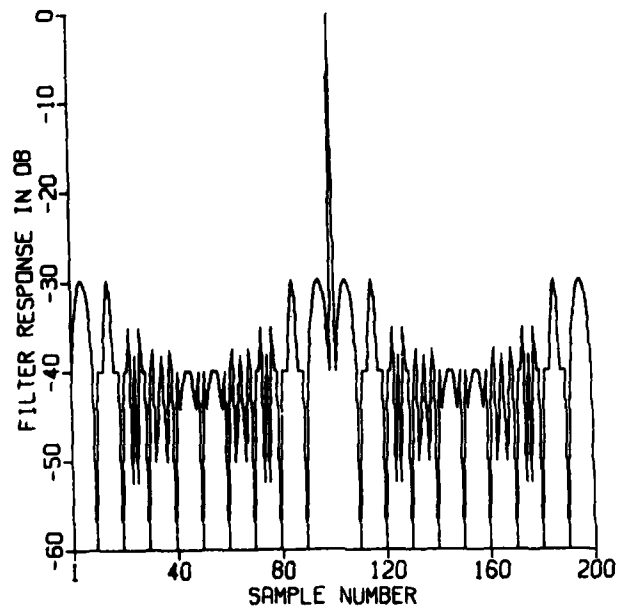


Fig. 4 — Frank code autocorrelation function,  $\rho = 100$ , zero doppler shift and no bandwidth limitation

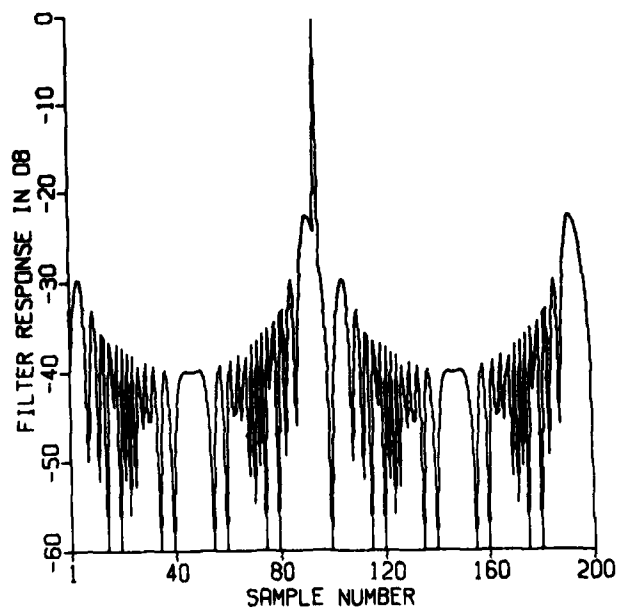


Fig. 5 — P3 or P4 autocorrelation function,  $\rho = 100$ , doppler = 0.05B with no bandwidth limitation

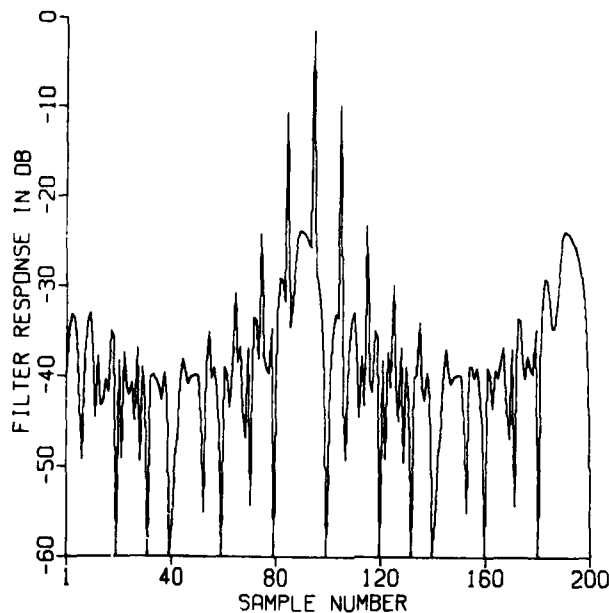


Fig. 6 — Frank code autocorrelation function,  $\rho = 100$ ,  
doppler = 0.05B with no bandwidth limitation

## CONCLUSIONS

The P3 and P4 polyphase, pulse-compression codes do not produce the large range-time grating lobes with large doppler shifts that are characteristic of the Frank, P1, and P2 codes.

Both the P3 and P4 codes can be compressed with digital fast Fourier transform circuits (FFT) with additive phase shifts in the FFT time samples and  $\pi$  phase shifts in every other FFT output (frequency) port.

The P4 code is much more tolerant of precompression bandwidth limiting than the P3 code.

The digitally implemented phase coding and compressing makes larger pulse compression ratios possible than would be feasible with dispersive delay line analog systems. In addition, the better doppler tolerance of the P3 and P4 codes permit these large time-bandwidths to be effective in the presence of large doppler-shifts on echo pulses.

## REFERENCES

1. Lewis, B. L. and Kretschmer, F. F., Jr., "A New Class of Pulse Compression Codes and Techniques" NRL Report 8387, Mar. 1980.
2. Lewis, B. L. and Kretschmer, F. F., Jr., "A New Class of Polyphase Pulse Compression Codes and Techniques," *IEEE Transactions on Aerospace and Electronic Systems*, AES-17, (3), May 1981, pp. 364-371.
3. Frank, R. L. (1963) "Polyphase Codes With Good Nonperiodic Correlation Properties", *IEEE Transactions on Information Theory*, Jan. 1963, IT, pp. 43-45.
4. Skolnik, M. I., *Radar Handbook* McGraw-Hill Inc., New York, 1970, pp. 35-15 and 35-16.

END

DATE  
FILMED

12-81

DTIC